THE JOURNAL OF PHYSICAL CHEMISTRY Letters

pubs.acs.org/JPCL

Highly Luminescent Mn-Doped ZnS Nanocrystals: Gram-Scale Synthesis

Bhupendra B. Srivastava,[†,‡] Santanu Jana,[†,‡] Niladri S. Karan,[†,‡] Sayantan Paria,[§] Nikhil R. Jana,[†] D. D. Sarma,[∥] and Narayan Pradhan*[,†,‡]

[†]Centre for Advanced Materials, [‡]Department of Materials Science, and [§]Department of Inorganic Chemistry, Indian Association for the Cultivation of Science, Jadavpur, 700032 India, and [∥]Solid State and Structural Chemistry Unit, Indian Institute of Science, Bangalore, 560 012 India

ABSTRACT Following growth doping technique, highly luminescent (quantum yield > 50%) Mn-doped ZnS nanocrystals are synthesized via colloidal synthetic technique. The dopant emission has been optimized with varying reaction parameters and found the ratio of Zn to S as well as the percentage of introduced dopant in the reaction mixture are key factors for controlling the intensity. The method is simple, hassle free, and can be scalable to gram level without hindering the quality of nanocrystals. These nanocrystals retain their emission during various ligand exchange processes and aqueous dispersion.

SECTION Nanoparticles and Nanostructures

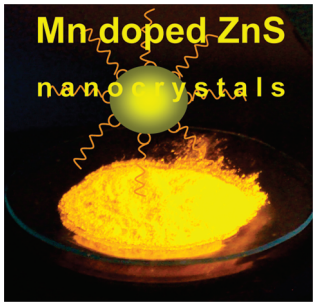

Light emitting semiconductor nanocrystals (quantum dots) have been widely investigated during the last two decades in view of their size-tunable optical properties, wide range of excitations, emission color purity, high quantum efficiency,[1,2] and their applications as a light emitting source in various opto-electrical devices and in biological applications.[3−6] The most investigated quantum dots are often cadmium-based materials, which have well developed synthetic chemistry and widely documented physical properties.[1−3] However, these nanocrystals are not suitable for widespread applications, as these contain Cd, a heavy metal, and are consequently toxic.[7] In recent developments, high-quality doped semiconductor nanocrystals are being explored as viable alternatives to undoped nanocrystals with additional advantages such as larger Stokes shift to avoid self-absorption, enhanced thermal and environmental stabilities, and minimized toxicity.[8−12] Different synthetic techniques and mechanistic studies for these doped semiconductor nanocrystals are already studied and reported in the literature.[8−15] The Mn-doped semiconductor system is one of the most studied among them.[8−11,13−20] Once Mn ions are doped in a semiconductor system, the exciton generated by photoexcitation of the host nanocrystal recombines via the lower lying states of the Mn^{2+} ion ($^4T_1-^6A_1$).[11,13,17] This leads to optical emission characteristic of Mn^{2+}, which is relatively independent of the nanocrystal size. In view of possible technological applications of such emission, there has been a sustained effort for more than a decade to enhance the dopant emission intensity from doped nanocrystals such as ZnS, ZnSe, and $Zn_{1-x}Cd_xS$ hosts.[8−11,16,18] The first high-intensity Mn emission was reported in ref 11 based on a Mn-doped ZnSe system, which achieved 22% quantum yield (QY).[11] Subsequent efforts have led to slightly more than 50% QY for the same system.[8,9] Surprisingly, there has been little progress in optimizing the QY of Mn emission from dispersed colloidal Mn-doped ZnS nanocrystals, although this system, besides being free from Se, was reported with a reasonably high QY (18%)[13] way before Mn-doped ZnSe was investigated. Using alloyed $Zn_{1-x}Cd_xS$[16] and core/shell CdS/ZnS hosts,[14] the QY from a sulfide semiconductor could be pushed up to about 25% and 50%, respectively. A very recent publication has reported a QY of ~35% for Mn-doped ZnS following a synthetic protocol similar to that reported in refs 8 and 9 with high percentage of dopant Mn.[18] The synthesis of Mn-doped ZnS nanocrystals with comparable QY to Mn:ZnSe- or undoped CdSe-based quantum dots is technologically important since Mn-doped ZnS is a greener material, free from both Cd and Se.

We report here large-scale synthesis of high-quality Mn-doped ZnS nanocrystals with more than 50% photoluminiscence (PL) QY using common and inexpensive chemicals following a simple and reproducible synthetic technique. Unlike the nucleation doping strategy, which has been developed for best emitting Mn-doped ZnSe[8,9] and later followed for Mn-doped ZnS as stated earlier,[18] our method follows a growth doping[19] technique where a minimum amount of dopants are introduced in the host to obtain intense dopant emission. The dopant emission has been optimized with varying reaction parameters, and it has been found that the ratio of Zn to S as well as the percentage of introduced dopant in the reaction mixture are key factors for controlling the intensity. The emission intensity of these doped nanocrystals is found to be stable under UV irradiation, ligand exchanges, and in water dispersions. It is further established that this

Received Date: March 23, 2010
Accepted Date: April 15, 2010

DOI: 10.1021/jz100378w | *J. Phys. Chem. Lett.* **2010**, *1*, 1454–1458

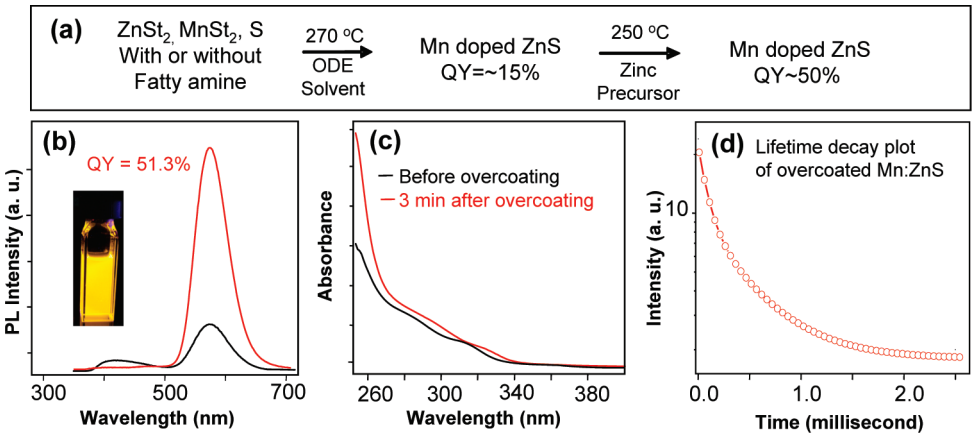

Figure 1. (a) Schematic presentation of the synthesis of Mn-doped ZnS nanocrystals with above 50% QY. (b,c) PL and UV−visible spectra of Mn-doped ZnS before (black) and after (red) the overgrowth of ZnS layers, respectively. (Inset) Digital picture of Mn-doped ZnS in chloroform excitation by a 254 nm UV lamp (6 mW)). Excitation wavelength is 320 nm for panel b. (d) Excited-state lifetime decay plot (in logarithmic scale, Y axis) of the sample after overcoating.

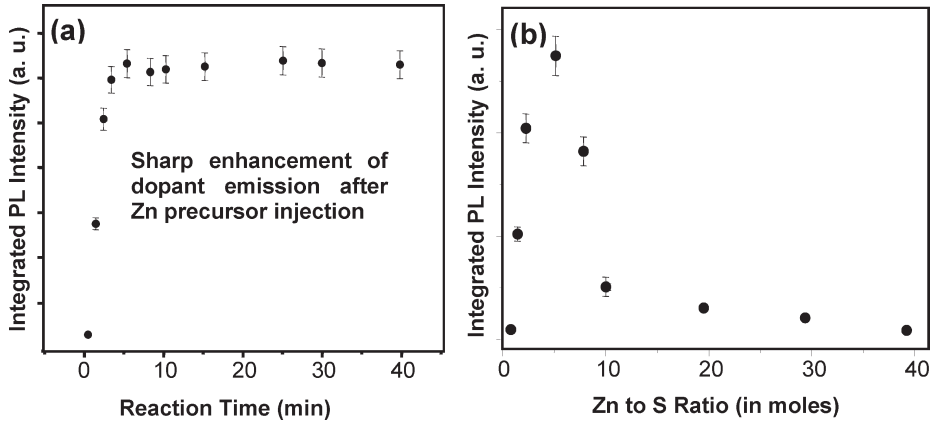

Figure 2. (a) Enhancement in the PL intensity (centered at 585 nm) with increasing annealing time after second-phase injection of zinc precursors to Mn-doped ZnS nanocrystals. (b) Variation of PL intensity with varying the initial ratio of Zn to S concentration.

approach is also efficient in doping Cu^{2+} ions into ZnS nanocrystals, leading to tunable blue-green emissions, suggesting the possibility of generalizing this approach.

The synthetic method is schematically shown in Figure 1a where all precursors (zinc stearate ($ZnSt_2$), manganese stearate ($MnSt_2$), and elemental S) along with the capping agent long-chain amine and solvent 1-octadecene (ODE) were loaded in a three-necked flask and heated to 270 °C under argon flow. Within 2−3 min, the Mn dopant emission evolves and intensifies with the reaction time reaching about 10−15% QY. However, this emission additionally exhibits a lower intensity broad emission centered at ~420 nm (Figure 1b, black line), presumably due to surface trap emissions. Further injection of excess zinc precursor to an "S"-rich reaction mixture at a slightly reduced temperature (250 °C) removes this broad emission and enhances the dopant emission, leading to more than 50% QY. This injection of $ZnSt_2$ was carried out in the presence of excess free stearic acid to avoid the formation of new nucleation of ZnS nanocrystals, and it also restricts the possible formation of ZnO.[20] The PL and corresponding UV−visible spectra before and after injection of the second lot of zinc precursor at 250 °C are shown in Figure 1b,c, respectively. The minimal shifting of band edge in the UV−visible spectra toward longer wavelength after adding excess Zn ions indicates the growth of ZnS nanocrystals. The excited-state lifetime (Figure 1d) in milliseconds (0.37) related to this dopant emission centered at ~585 nm obtains its origin from the manganese center as reported in the literature.[18]

Figure 2a shows the dopant emission intensity versus annealing time after the injection of the second lot of $ZnSt_2$; the plot clearly shows a rapid increase of dopant emission intensity that goes beyond 50% QY within 3 min of injection. In a typical reaction, the QY of the final dopant emission was found to be 51.3% (Supporting Information) in chloroform for 1% dopant Mn^{2+} ion (to the Zn concentration). This enhancement in emission is possibly driven by the fact that nonemissive surface Mn ions are covered by the over growth of a thin layer of ZnS generating a proper tetrahedral environment for Mn ions. Further growth does not improve the emission efficiency but helps for better stability. We have performed a series of reactions to test the reproducibility of the QY, and it

DOI: 10.1021/jz100378w | J. Phys. Chem. Lett. 2010, 1, 1454–1458

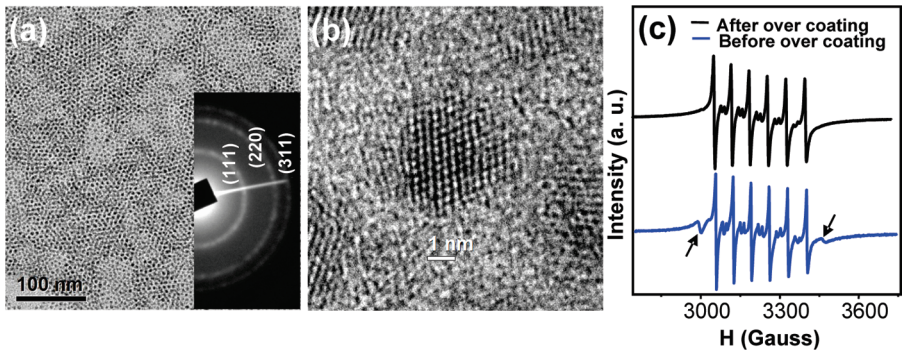

Figure 3. (a) Large-area TEM micrograph of nearly monodispersed Mn-doped ZnS nanocrystals. Inset is the diffraction pattern showing their cubic structure. (b) HRTEM image of a Mn-doped ZnS nanocrystal. (c) EPR of Mn-doped ZnS before overcoating (blue) and after overcoating (black) with a shell of ZnS.

was found that the average sample gives 35−40% QY as measured using quinine sulfate dye.

To understand such exceptionally high PL QY in this system, we carried out systematic variations in the reaction system and found controlled nucleation; doping and growth processes with proper manipulation of reaction parameters and reactant concentrations are the root cause for such intense dopant emission. The amount of Mn precursor (optimally ∼1% of the host) and the ratio of initial Zn and S precursors are the two most critical quantities responsible for such an efficient emission. The presence of a higher amount of Mn precursor reduces the dopant intensity (Figure S1), and a limited amount of S facilitates ZnO formation as observed from X-ray diffraction (XRD; data not shown). There is a fast increase in the QY for the Zn to S ratio increasing from 1:1 to 1:5 followed by a steep decrease until a Zn to S ratio of 1:10 is reached, followed by a slower decrease (Figure 2b). The amount of S precursor here balances the reactivity of the Zn and Mn precursors. $MnSt_2$ always needs more S than $ZnSt_2$ to form its respective sulfide, and hence the proper ratio of all precursors in a one-pot system is required for efficient dopant emission. Varying the S concentration, here we have optimized the best possible doping conditions to obtain high-quality Mn-doped ZnS nanocrystals. Excess amount of S (10 times the Zn amount) helps the host nanocrystal grow faster and also creates a large amount of host nucleation, which slows down the incorporation of dopant Mn ions. Hence the dopant emission QY reduces drastically with higher anion S concentration. The detailed synthetic procedure with variation of different parameters is presented in the Supporting Information.

Figure 3a shows a transmission electron microscopy (TEM) image after the final growth of the nanocrystal (3.8 ± 0.2 nm, high-resolution TEM (HRTEM), Figure 3b) while Figure S2 shows the TEM micrograph of Mn-doped ZnS (∼3.2 ± 0.4 nm) nanocrystals before the overcoating with the second lot of zinc precursor. These nanocrystals are nearly monodispersed, exhibiting cubic crystal structure confirmed by XRD (Figure S3). Electron paramagnetic resonance (EPR) spectra of purified samples before and after injection of Zn precursor are shown in Figure 3c. The hyperfine coupling constant, $A = 69.2$ G from our final sample (black line) agrees well with the hyperfine coupling constant obtained for Mn at cubic ZnS lattice sites in bulk ZnS[11] ($A = 69.6$ G). EPR data recorded prior to overcoating of the doped nanocrystals by the addition of Zn precursor (blue line) exhibits a very similar characteristic pattern. However, an additional peak in the lower and higher magnetic field can be clearly observed in this case, marked by arrows in the figure. This suggests that a small fraction of Mn^{2+} ions are present on the surface of ZnS nanocrystals. The disappearance of this spectral feature on further addition of excess Zn precursor confirms the formation of an effective shell of ZnS, which places these surface Mn^{2+} ions inside the shell of doped ZnS nanocrystals.

The present simple synthetic approach leads to several advantages in addition to the high PL QY and the use of environmentally friendly, greener precursor materials. Interestingly we found that this synthetic technique can be easily scaled up to gram-level production (Figure S4) of the sample while still retaining QY >30%, making this synthetic technique an ideal approach for industrial production.

These nanocrystals are phase transferred to water using poly(acrylic acid), mercaptocarboxylic acid (MPA), cystamine hydrochloride ligands, and so forth (Supporting Information), which retained almost the entire dopant emission intensity in their aqueous dispersion. These highly luminescent nanocrystals in water are found to be stable for months in ambient conditions. Figure 4a shows UV−visible and PL spectra of MPA-capped Mn-doped ZnS in water with 35% QY, which is good enough for different applications including biological labeling.

Another aspect of this synthetic approach is the possibility of its generalization to dope other transition metal ions into such semiconductor nanocrystal hosts. We have extended Cu^{2+} ion doping in ZnS nanocrystals (Figure 4b). The QYs of such emissions remain approximately 5% in solution. Doping of Cu^{2+} ions in a ZnS nanocrystal host needs further optimization to obtain highly efficient Cu-doped ZnS nanocrystals, although this much QY for this Cu doped sample is also very encouraging.

In conclusion, we report here a new and rather simple synthetic route to achieve bright, stable, and efficient emission from Mn-doped ZnS nanocrystals with considerably improved optical properties than earlier reports. Importantly, the synthetic method can be upscaled to gram-level preparation of doped nanocrystals without compromising their

DOI: 10.1021/jz100378w | J. Phys. Chem. Lett. 2010, 1, 1454–1458

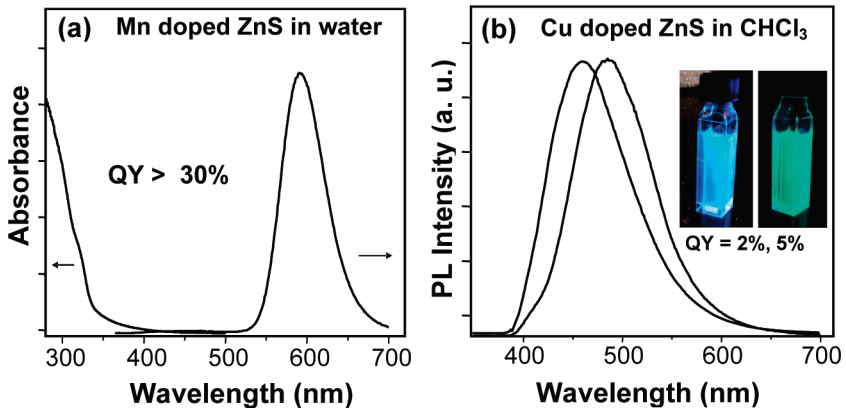

Figure 4. (a) Typical UV−visible and PL spectra of water-soluble Mn-doped ZnS nanocrystals. (b) Tunable PL spectra of Cu^{2+}-doped ZnS nanocrystals in chloroform synthesized by a similar synthetic technique. Excitation wavelength is 320 nm. The QYs of the resulting samples are low but are found to be stable in air for months. Insets are digital images of Cu^{2+}-doped ZnS nanocrystals excited at 254 nm.

quality and emission property. It is found that these samples can be transferred to water by all usual methods while retaining high QY. Importantly, the reproducible and simple synthetic approach would enable its synthesis in a common laboratory. Based on greener and nontoxic materials, this synthetic method is also found to effectively dope Cu^{2+} in the same nanocrystal host, giving blue and green color emissions and suggesting the possibility of generalization of this method.

SUPPORTING INFORMATION AVAILABLE Details of materials used, experimental techniques, instrumentations, determination of QY, and XRD of Mn-doped ZnS. This information is available free of charge via the Internet at http://pubs.acs.org.

AUTHOR INFORMATION

Corresponding Author:

*To whom correspondence should be addressed. E-mail: camnp@iacs.res.in.

ACKNOWLEDGMENT B.B.S., S.J., and N.S.K. acknowledge CSIR of India for Research Fellowship, and DST of India is acknowledged for funding. D.D. acknowledges JC Bose, and N.P. acknowledges LNJ Bhilwara for Fellowship.

REFERENCES

(1) Murray, C. B.; Norris, D. J.; Bawendi, M. G. Synthesis and Characterization of Nearly Monodisperse CdE (E = Sulfur, Selenium, Tellurium) Semiconductor Nanocrystallites. *J. Am. Chem. Soc.* **1993,** *115*, 8706–8715.

(2) Peng, Z. A.; Peng, X. Nearly Monodisperse and Shape-Controlled CdSe Nanocrystals via Alternative Routes: Nucleation and Growth. *J. Am. Chem. Soc.* **2002,** *124*, 3343–3353.

(3) Alivisatos, A. P. Semiconductor Clusters, Nanocrystals, and Quantum Dots. *Science* **1996,** *271*, 933–937.

(4) Coe, S.; Woo., W. K.; Bawendi, M. G.; Bulovic, V. Electroluminescence from Single Monolayers of Nanocrystals in Molecular Organic Devices. *Nature* **2002,** *420*, 800–803.

(5) Medintz, I. L.; Uyeda, H. T.; Goldman, E. R.; Mattoussi, H. Quantum Dot Bioconjugates for Imaging, Labelling and Sensing. *Nat. Mater.* **2005,** *4*, 435–446.

(6) Talapin, D. V.; Murray, C. B. PbSe Nanocrystal Solids for n- and p-Channel Thin Film Field-Effect Transistors. *Science* **2005,** *310*, 86–89.

(7) Kirchner, C.; Liedl, T.; Kudera, S.; Pellegrino, T.; Javier, A. M.; Gaub, H. E.; Stoelzle, S.; Fertig, N.; Parak, W. J. Cytotoxicity of Colloidal CdSe and CdSe/ZnS Nanoparticles. *Nano Lett.* **2005,** *5*, 331–338.

(8) Pradhan, N.; Goorskey, D.; Thessing, J.; Peng, X. An Alternative of CdSe Nanocrystal Emitters: Pure and Tunable Impurity Emissions in ZnSe Nanocrystals. *J. Am. Chem. Soc.* **2005,** *127*, 17586–17587.

(9) Pradhan, N.; Peng, X. Efficient and Color-Tunable Mn-Doped ZnSe Nanocrystal Emitters: Control of Optical Performance via Greener Synthetic Chemistry. *J. Am. Chem. Soc.* **2007,** *129*, 3339–3347.

(10) Norris, D. J.; Efros, A. L.; Erwin, S. C. Doped Nanocrystals. *Science* **2008,** *319*, 1776–1779.

(11) Norris, D. J.; Yao, N.; Charnock, F. T.; Kennedy, T. A. High-Quality Manganese-Doped ZnSe Nanocrystals. *Nano Lett.* **2001,** *1*, 3–7.

(12) Jana, S.; Srivastava, B. B.; Acharya, S.; Santra, P. K.; Jana, N. R.; Sarma, D. D.; Pradhan, N. Prevention of Photooxidation in Blue−Green Emitting Cu Doped ZnSe Nanocrystals. *Chem. Commun.* **2010,** *46*, 2853–2855.

(13) Bhargava, R. N.; Gallagher, D.; Hong, X.; Nurmikko, A. Optical Properties of Manganese-Doped Nanocrystals of Zinc Sulfide. *Phys. Rev. Lett.* **1994,** *72*, 416–419.

(14) Yang, Y.; Chen, O.; Angerhofer, A.; Cao, Y. C. Radial-Position-Controlled Doping in CdS/ZnS Core/Shell Nanocrystals. *J. Am. Chem. Soc.* **2006,** *128*, 12428–12429.

(15) Archer, P. I.; Santangelo, S. A.; Gamelin, D. R. Inorganic Cluster Syntheses of TM^{2+}-Doped Quantum Dots (CdSe, CdS, CdSe/CdS): Physical Property Dependence on Dopant Locale. *J. Am. Chem. Soc.* **2007,** *129*, 9808–9818.

(16) Nag, A.; Chakraborty, S.; Sarma, D. D. To Dope Mn^{2+} in a Semiconducting Nanocrystal. *J. Am. Chem. Soc.* **2008,** *130*, 10605–10611.

(17) Soo, Y. L.; Ming, Z. H.; Hunag, S. W.; Kao, Y. H.; Bhargava, R. N.; Gallagher, D. Local Structures around Mn Luminescent Centers in Mn-Doped Nanocrystals of ZnS. *Phys. Rev. B: Condens. Matter* **1994,** *50*, 7602–7.

(18) Zheng, J.; Yuan, X.; Ikezawa, M.; Jing, P.; Liu, X.; Zheng, Z.; Kong, X.; Zhao, J; Masumoto, Y. Efficient Photoluminescence

DOI: 10.1021/jz100378w | *J. Phys. Chem. Lett.* **2010,** *1*, 1454–1458

of Mn^{2+} Ions in MnS/ZnS Core/Shell Quantum Dots. *J. Phys. Chem. C* **2009,** *113*, 16969–16974.

(19) Acharya, S.; Sarma, D. D.; Jana, N. R.; Pradhan, N. An Alternate Route to High-Quality ZnSe and Mn-Doped ZnSe Nanocrystals. *J. Phys. Chem. Lett.* **2010,** *1*, 485–488.

(20) Yang, Y.; Angerhofer, A.; Cao, Y. C. Radial-Position-Controlled Doping of CdS/ZnS Core/Shell Nanocrystals: Surface Effects and Position-Dependent Properties. *Chem.—Eur. J.* **2009,** *15*, 3186–3197.

DOI: 10.1021/jz100378w | *J. Phys. Chem. Lett.* **2010,** *1,* 1454–1458